Available online at www.sciencedirect.com
SCIENCE DIRECT®
Journal of Sound and Vibration 274 (2004) 163–192
JOURNAL OF SOUND AND VIBRATION
www.elsevier.com/locate/jsvi

Smart panel with multiple decentralized units for the control of sound transmission. Part I: theoretical predictions

P. Gardonio*, E. Bianchi, S.J. Elliott

Institute of Sound and Vibration Research, University of Southampton, Highfield, Southampton SO17 1BJ, UK

Received 29 November 2002; accepted 20 May 2003

Abstract

This is the first of three companion papers that summarize the theoretical and experimental work carried out to develop a prototype smart panel with 16 decentralized vibration control units for the reduction of sound radiation/transmission. The smart panel is made of a thin aluminium plate with 16 closely spaced accelerometer sensor and piezoceramic actuator transducer pairs connected by single-channel velocity feedback controllers (i.e., active damping units). In this paper a preliminary theoretical study is carried out to assess the behaviour of the smart panel when it is mounted on the top of a rectangular cavity with rigid walls. The smart panel is excited either by the acoustic field produced in the cavity by a monopole source or by a transverse point force. The simulations carried out have shown that for both the acoustic and the force sources, good reductions of the averaged kinetic energy or total sound power radiation can be achieved within a band 0–2 kHz.

The theoretical study is preceeded by a general review of the development of smart panels for the control of sound radiation/transmission. In particular, the various approaches developed for the design of sensors and actuators are analyzed with reference to the control of tonal disturbances using feed-forward controllers and the control of stationary random disturbances using feedback controllers.

1. Introduction

This is the first of three companion papers that summarize the theoretical and experimental work carried out to develop a prototype smart panel with 16 decentralized vibration control units for the reduction of sound radiation/transmission [1,2]. Starting from the very promising results obtained in the simulation study of Elliott et al. [3], a prototype panel has been designed, built and tested. In this paper a preliminary theoretical study is presented of the behaviour of the smart

*Corresponding author. Tel.: +44-23-8059-4933; fax: +44-23-8059-3190.
E-mail address: pg@isvr.soton.ac.uk (P. Gardonio).

0022-460X/$ - see front matter
doi:10.1016/j.jsv.2003.05.004

panel when it is mounted on the top of a rectangular cavity with thick rigid walls. This particular configuration has been chosen to simplify the experimental work, which involves measuring the sound radiation of the panel due to either a primary acoustic source (a loudspeaker) within the cavity or a primary structural source (a shaker) acting on the panel.

This paper is structured into three parts. In Section 2 the various stages of the development of smart panels for the control of sound radiation/transmission is examined. The objective of this review is to highlight how and why scientists have developed two different control approaches. In the first approach the aim is to rearrange the vibration field of the panel in order to reduce the sound radiation at specific narrow frequency bands using feed-forward control systems. The aim of the second approach is to damp the vibration of the panel at resonant frequencies using feedback control systems so that random disturbances can be controlled within relatively large bands at low frequencies where the sound radiation is governed by the resonances of the panel.

Sections 3 and 4 describe the smart panel with the 16 decentralized control units and present the mathematical model that has been used to study the sound radiation/transmission of the smart panel when mounted on the rectangular cavity. The dynamic effects of the sensor (accelerometer) and actuator (piezoceramic[1] patch) components of each control unit have been modelled in detail. In this way it has been possible to present in the second companion paper [2] an accurate analysis of the stability/performance of the 16 channels velocity feedback control systems.

In Section 5 simulations results are presented where the control effectiveness of the smart panel under study is assessed in terms of the reduction of the kinetic energy or sound radiation/transmission in a frequency band between 0 and 2 kHz. This analysis has been carried out for both the acoustic primary disturbance in the rectangular cavity (monopole acoustic source) and the vibratory primary disturbance on the panel (transverse point force). Also the average reductions, in a frequency band between 0 and 2 kHz, are given for both the kinetic energy and sound radiation/transmission with reference to the control gains implemented in the 16 decentralized velocity feedback control systems.

2. Smart panels for the control of sound radiation/transmission into enclosures

Active noise control (ANC) and *active noise and vibration control* (ANVC) systems have given successful results for the control of tonal noise disturbances in relatively small enclosures such as the cabins of propeller aircraft or cars as described in Chapter 10, "Global Control of Enclosed Sound Fields", of Ref. [4]. These control systems operate with large numbers of error sensors and actuators scattered within the cavity via a *multi-input multi-output* (MIMO) adaptive *feed-forward* controller [4]. Therefore they are relatively bulky, heavy, invasive and costly systems that can control only tonal disturbances for which a causal reference signal unaffected by any control input could be fed through to the controller. As a result they have been successfully implemented only in few applications, such as the control of tonal disturbances in propeller aircrafts Refs. [4, Section 10.15; 5–8] or engine noise in cars Refs. [4, Section 10.15; 9,10].

ANC systems using adaptive feed-forward controllers have also been developed for the control of stationary random disturbances. The success of these control systems depends on two issues:

[1] PZT: led, zirconate, titanate.

first, the possibility of modelling within the controller the feedback effects of the secondary sources on the reference sensors so that the control filters can be derived from the design of an optimal dummy controller and, second, the possibility of measuring the primary disturbance well in advance so that the optimal controller has a causal impulse response [4]. These two problems have made the development of ANC or ANVC systems very difficult and challenging either for the control of jet or air flow stationary random noise in aircraft [11,12] or the control of road and aerodynamic stationary random noise in cars [13,14]. Up to the present, the only really successful application has been for the control of random fan noise in ventilation ducts, where the reference signal can be taken sufficiently far in advance to guarantee a causal optimal filter and the feedback effect of the control sources on the detection sensors can be clearly identified [4,15].

2.1. Feed-forward active structural acoustic control

During the past two decades scientists have begun to consider the possibility of reducing noise transmitted to enclosures by actively controlling the sound radiation/transmission through the side walls. In this case structural actuators are integrated on the walls in such a way as to modify the vibration of the partitions and thus reduce the sound radiation/transmission. A detailed introductory description of this method, also known as *active structural acoustic control* (ASAC), is given in Ref. [16, Chapter 8]. This control approach was conceived and initially developed within the same scientific community that studied ANC systems. As a result the first ASAC systems were built using adaptive feed-forward controllers which (a) require a set of error sensors scattered in the receiver room for the detection of the total sound power radiation as an error parameter to be minimized and (b) enable only the control of tonal disturbances for which a causal reference signal could be fed through to the controller [16,17]. Thus, although the actuators were integrated on the walls, these systems still had all the practical drawbacks listed for ANC and AVNC systems. Moreover, it was found that, in some frequency bands, the minimization of the sound radiation was achieved by reconstructing the modal response of the partition so that the vibration field was slightly enhanced rather than reduced, with consequent potential problems related to mechanical failure [16–20]. This phenomenon was found to be caused by the sound radiation mechanism. Above the critical frequency [21], the sound radiation of a partition is determined only by the self-radiation efficiency of each structural mode, and these self-radiation efficiencies are independent to the modal order [22]. In contrast, below the critical frequency the sound radiation of a partition is controlled both by the self-radiation of each structural mode and by the mutual radiation of pairs of structural modes, the self- or mutual radiation efficiencies also depend heavily on the mode orders (in general structural modes with both or one odd mode order have greater radiation efficiencies and the radiation efficiency tends to decrease as the mode order is increased) [21–23]. This detailed description of the sub-critical behaviour is necessary unless the resonance frequencies of the partition are well separated [24]. The overall vibration of the partition when it has well separated resonance frequencies is primarily controlled by the resonant structural modes and thus the sound radiation is governed by the self-radiation efficiencies of the resonant structural modes themselves [16,22]. However, either at off-resonance frequency bands or at higher frequencies, where the modal overlap of the partition is sufficiently high so that several resonant modes determine its vibration [24], the sound radiation contribution due to the mutual effects of a pair of modes is not negligible [16,22,23]. Although the self-radiation resistance

of each structural mode is always positive, the mutual radiation resistance of pairs of structural modes could assume negative values which give rise to sound cancelling effects [22]. Thus, below the critical frequency, the control system can reduce the total sound power radiated/transmitted in narrow frequency bands by rearranging the vibration contribution of each single structural mode in order to maximize this sound cancelling effect. This approach is termed *modal restructuring* [19] which could even result in a small enhancement of the vibration level of the partition [16,18–20]. Alternatively, at resonance frequencies of well separated structural modes or at frequencies above the critical frequency, the control system can reduce the total sound power radiated only by reducing the vibration contribution of efficiently radiating structural modes. This approach is termed *modal suppression* [19]. Burdisso and Fuller [25] considered the modal restructuring mechanism from a different point of view, where the vibration of the structure after control is characterized by new eigenvalues and eigenfunctions which have lower radiation efficiencies.

An important step forward for this technology was achieved by integrating error sensors within the partition which were able to estimate the farfield sound radiation [26–33]. This allowed the construction of compact and light control systems with a relatively small number of input–output channels that were therefore more suitable for practical applications. Most of this research arose from the aerospace and naval sectors where there was a clear requirement for reducing the structure-borne noise transmission or radiation of the fuselage walls or marine hull which are generally made of thin and lightly damped panels [34]. It was found that, at relatively low frequencies where the acoustic wavelength is larger than the dimensions of the panels that make up the fuselage walls or marine hull, the vibration of each panel can be considered to be the superposition of a number of frequency-dependant self-radiating *radiation modes*, of which by far the most efficient one closely corresponds to the net *volume velocity* of the panel over a relatively large frequency band [32,35] (for more details see Refs. [32]). A lot of work has therefore been carried out to develop *smart panels* with integrated distributed strain sensors [31,35–51] or with arrays of sensors [49–60] that measure the vibration components of a panel that mostly contribute to the farfield sound radiation, in particular the first radiation mode and the volumetric vibration of the panel [35]. Active control tends to be effective at relatively low frequencies where the first radiation mode, or its volume velocity approximation, produces most of the sound radiation. Thus, the output of just one error sensor can provide a good estimate of the total sound radiation by a panel.

Work has also been carried out to build single-input strain actuators, made either with arrays of small piezoceramic patches or distributed piezoelectric films [36,39,41,49–52,61–70], that efficiently couple with the sensor transducer. If the sensor–actuator transducers are collocated[2] and dual[3] [51,71–74] then the real part of their response function is constrained to be positive real, so that a single-input single-output (SISO) adaptive feed-forward controller could be implemented with a very fast-acting controller [35]. Thus the technological progress in the construction of smart panels with collocated and dual sensor–actuator pairs has given the possibility of building very

[2] Collocation is a geometrical condition where point sensors and actuators are placed in the same position of the structure and distributed sensors and actuators with equal spatial sensitivity are placed over the same area of the structure.

[3] Duality is a physical property were the actuator and sensor excites and detects the vibrations of a structure in the same manner so that the product of the excitation and sensed response is proportional to the power supplied to the system. Dual sensor–actuator pairs are also said to be "matched," "compatible" or "reciprocal."

compact, light and non-invasive control systems that could be very effective for the control of tonal disturbances [16,28–33].

Some attempts have also been made to develop adaptive feed-forward controllers for broadband random disturbances by placing detection sensors in the vicinity of the panel if not on the panel itself [75]. In this case the main problem is caused by the fact that having closely placed detection sensor and control actuator transducers prevents the possibility of deriving a causal controller [76]. This type of control system has been developed with some level of success in double-panel partitions, such as aircraft double-wall constructions, by placing the detection transducers on the excited panel and the control and error transducers on the radiating panel [77].

2.2. Feedback active structural acoustic control

In parallel to the work on ASAC systems with feed-forward controllers, research was also carried out to develop ASAC systems using feedback controllers. The implementation of feedback control systems does not require a reference signal so that, when used for disturbance rejection applications, they could be used equally to control tonal and random, wide-band, disturbances. Baumann et al. [26] and Baumann and Robertshaw [27] first proposed a methodology to design a feedback control system for the reduction of broadband sound radiation by a panel which uses structural error sensor and control actuator transducers acting on the panel. Their instructive work has originated several studies where MIMO feedback control systems using structural sensors and actuators have been used in smart panels for the control of sound radiation/transmission. The background of most of the scientists that developed these control systems was modern feedback control theory where the synthesis of the optimal feedback gains in the controller is made using a state-space formulation [50,51]. A series of papers have therefore been published where optimal *static*- (fixed gains) or *dynamic*- (frequency-dependent gains) *controllers* are designed with reference to H_2 or H_∞ cost functional that refer to either a set of states of the system (*state-feedback*) or a set of measured output parameters (*output-feedback*) [26,27,50,51,78–86]. Work has also been presented where the optimal controller has been derived from the standard *linear quadratic regulator* (LQR) or *linear quadratic Gaussian* (LQG) problems which however could be considered as a subset of the more general H_2 optimization problem [50,51,87,88]. A consistent review of the various aspects that characterize the modern approach for the design of feedback controllers for vibration/sound-radiation rejection problems is given in Refs. [50,51].

Although most of the initial studies have demonstrated the possibility of designing MIMO state-feedback control systems for ASAC purposes, the implementation stage has resulted in a series of practical problems. For example, in order to have compact smart panels, the parameter to be controlled, the radiated sound power, is not directly measured but derived from a set of structural sensors bonded on the panel. From the control point of view this means that the performance variables, i.e. the states, of the systems cannot be directly measured and thus output-feedback controllers cannot be implemented. As a consequence state-feedback control has to be implemented that requires a *state estimator* or *observer* system which models the essential physics of the system. In practice, the state estimator consists in a set of analogue or digital filters which model the plate dynamics and the sound radiation mechanisms as suggested by Baumann et al. [26] and Baumann and Robertshaw [27].

2.3. Feedback SISO active structural acoustic control

Although the work carried out to develop distributed strain sensors and actuators for smart panels was initially aimed toward the implementation of feed-forward control systems, scientists soon recognized that these types of transducers would also have great advantages in the design and implementation of feedback control systems. Indeed the possibility of building strain sensors which measure the radiation modes of panels has given the possibility of implementing output-feedback control systems where the state variables to be minimized could be directly derived from the measured radiation modes outputs without the need of a state estimator. In particular, since the low-frequency sound radiation is controlled by the first radiation mode, and knowing that, at relatively low frequencies, the first radiation mode could be approximated by the volume velocity vibration of the panel component which is frequency independent, the possibility of developing SISO feedback control systems was envisaged [32,35].

Classic feedback control theory has been used to design the sensor–actuator transducers for the implementation of simple SISO feedback control systems [89–92]. This control approach is characterized by the classic disturbance rejection feedback control loop, in which the output of the system, for example the volumetric vibration or a specific radiation mode of the panel, is the sum of the primary disturbance and the control excitation, that is itself proportional to the measured output via a feedback control function. Simple functions can be arranged to enhance the mass, stiffness and damping effects of the controlled structure. However for the specific case of disturbance rejection the most suitable strategy is *active damping*, which reduces the response of the structure at resonance frequencies and, as a result, the steady state response to wide-band disturbances [51]. Active damping does not produce control effects at off-resonance frequency bands but, on the contrary tends to fill-in the response spectrum at anti-resonance frequencies. Therefore, active damping is not particularly suitable for the control of tonal disturbances except in the particular case where the excitation frequency corresponds to a resonance frequency of the smart panel which does not vary as the physical or operative conditions changes (variation of temperature or change of static loading, etc.). The literature on classic feedback control is well established particularly for servo-mechanisms and a detailed summary of SISO classic feedback control theory of flexible structures is given in Refs. [50,51].

The simplest way of achieving active damping is by implementing *rate feedback* or *direct velocity feedback*. In this case the output of the sensor is directly fed back to the actuator via a fixed control gain. This control scheme is constrained to be stable for any value of the control gain if the sensor–actuator or "plant" frequency response is strictly positive real [35,50,51,70]. As highlighted in the previous sub-section, this happens when the sensor–actuator transducers are collocated and dual. Most of the work carried out by scientists is therefore focussed on the design of collocated and dual sensor–actuator pairs so that a relatively simple feedback controller which is unconditionally stable could be implemented [52]. If the sensor–actuator transducers are not collocated and dual then only a limited range of control gains could be implemented in order to guarantee stability and this results in a reduced performance capability of the system. In this case the control performance could be enhanced by shaping the control function with standard compensator circuits as for example *Lead*, *Lag*, *PI* and *PID* compensators.

Building distributed sensor–actuator transducers which are collocated and dual is not an easy task. The most obvious way of building these sensor–actuator pairs is by placing the sensor on one

side of the panel and the actuator on the opposite side of the panel. Gardonio et al. [70] have shown that in general this simple construction could not provide a strictly positive response function if the sensor output is determined by both the bending and in-plane vibration of the panel generated by the actuator. Although the in-plane vibration of the panel is relatively small compared to the bending one at low frequencies, the sensor output is severely affected by this component which produces an extra phase shift, at the first in-plane resonant mode of the panel. As a result at higher frequencies the sensor–actuator response function is not strictly positive real and is characterized by larger amplitude values than those corresponding to the low-frequency range of control. This precludes the implementation of direct velocity feedback control and even with an appropriate compensator circuit only small control gains could be implemented and thus small control effects are achieved. Several alternative constructions have been studied to avoid this sensor–actuator feed-through effect. For example, the distributed sensor has been substituted with a grid of accelerometers, although even in this system aliasing effects produce a non-positive real response function [57–60]. Alternatively, Lee et al. [93] have proposed the use of double-layer sensor–actuator transducers to be operated in such a way as to avoid the detection of in-plane vibration and to excite the plate only in bending. In this case the implementation of the two transducers is corrupted by interlayer coupling effects [93]. Cole and Clark [94] have proposed a similar solution where only two transducers are used, which work simultaneously as actuators and sensors. This solution avoids the interlayer coupling effect described above. However, the implementation of these sensori-actuators is not trivial since relatively small charge outputs have to be derived from the large inputs to each transducer. This requires compensation techniques which are very sensitive to physical or operative changes of the system (static loads, temperature, etc.). Finally the operation of relatively large distributed sensor or actuator transducers with shaped electrodes is relatively sensitive to shaping errors of the electrodes which could contribute to making the response function to be not strictly positive [95].

Some researchers developed a particular design approach for feedback systems, in which the control system can be modelled with a feed-forward control scheme. This was done by building an internal model of the control path in the feedback loop and so the approach has become known as *internal model control* IMC [96]. With this approach, the implementation of a feedback control scheme is redirected to the derivation of a suitable model of the feedback path and the derivation of a classic adaptive feed-forward control filter. The implementation of ASAC with IMC feedback control schemes has been tested in a few cases [97–99].

2.4. Decentralized MIMO feedback active structural acoustic control

The problems encountered in the development of smart panels with SISO feedback ASAC control using large-area distributed transducers have forced researchers to find alternative control solutions.

In Section 2.1 it was argued that below the critical frequency and for low frequencies such that the resonances of the panel are well separated, the sound radiation at resonance is controlled by the self-radiation efficiency of the resonant mode. In contrast, the off-resonance frequency sound radiation is controlled by both the self- and mutual-radiation efficiencies of the structural modes. A new formulation of the sound radiation in terms of radiation modes was therefore proposed as a tool to design structural sensors that would have been able to estimate the sound radiation either at resonance or off-resonance frequencies. Such complicated sensors are not necessary to

implement active damping feedback control. Active damping feedback control tends to be effective only in the vicinity of resonance frequencies, where the sound radiation is controlled by the self-radiation of the resonant mode, while it tends to enhance the vibration at anti-resonance frequencies, where the sound radiation is controlled by the self- and mutual-radiation effects of a set of modes. Therefore, in order to implement active damping feedback control, it is sufficient to have sensor–actuator transducers that are well coupled with the low order structural modes. Moving the sensor–actuator design problem from the control of radiation modes to that of structural modes is not a real improvement since distributed sensor and actuator transducers that cover the entire surface of the panel are still required. However Elliott et al. [3] have shown that active damping of structural modes could be achieved with small localized control units that implement SISO velocity feedback control. They initially considered the ideal case of having a collocated and dual point-velocity and point-force sensor–actuator system which is positioned away from the nodal lines of the modes to be controlled. These two transducers would enable the implementation of unconditionally stable direct velocity feedback control. Elliott et al. [3] noticed that as the control gain is gradually increased from zero, the active damping effect of the structural modes grows and consequently both the total kinetic energy and total sound radiation of the panel averaged in a certain frequency band decrease. However, they also found that this behaviour is only valid up to an optimal feedback control gain, above which the damping effect fades away and so the kinetic energy or sound radiation by the panel increases again and can even become larger than before control. The analysis of this phenomenon showed that the velocity feedback control unit works as a sky-hook damper which absorbs energy from the structural modes. However, for large control gains the action of the feedback controller is to pin the panel at the error sensor position, so that the vibration of the panel is that of a lightly damped structure with extra pinning points. Therefore a set of new lightly damped structural modes are created which could be excited at new resonance frequencies and radiate sound even more effectively than the original modes (see Section 2.5 of Ref. [21]).

Starting from these considerations Elliott et al. [3] proposed a new control configuration based on grids of decentralized velocity feedback control units using a piezoceramic patch actuator with a small accelerometer on the centre. Although it is non-collocated and non-dual, this sensor–actuator configuration enables relatively large feedback control gains so that the equivalent of a grid of sky-hook dampers could be implemented provided the control gains do not exceed the optimal values. The large number of control units, which are evenly scattered over the panel surface, allows the damping of a relatively large number of low-frequency resonant modes and consequently the low-frequency wide-band sound radiation control. This type of vibration and sound radiation control effects was first observed by Petitjean and Legrain [100] in an experiment where a grid of 5×3 collocated piezoceramic patches mounted on either side of a panel was used to implement either a fully coupled MIMO LQG feedback controller or fifteen SISO rate feedback controllers. For this particular type of panel they found that the vibration reductions in the two control cases were very similar. This type of experiment was then repeated on a different smart panel [101] and it was again found that, despite its simplicity, decentralized feedback control was giving similar control effects to those of a MIMO optimal feedback controller. Indeed Petitjean et al. [101] noted that "Whatever the control algorithm, in this experiment of active noise control, it turns out that controlling panel vibrations through distributed actuators and sensors results in an attenuation of the pressure field. This fact seems contradictory to some previously published studies on the topic, which point out

that it is important to take the radiation efficiency of the plate modes whose frequencies lie within the frequency band of interest into account in the control law.'' The contradiction comes from the fact that radiation mode theory is important when feed-forward active control is implemented at off-resonance frequencies where the mutual radiation effects cannot be neglected. Alternatively, active damping feedback control regulates the vibration at resonance frequencies where the sound radiation is determined only by the resonant modes.

3. System studied

The system studied in this paper is shown in Fig. 1 and consists of a clamped and baffled aluminium panel of dimensions $l_x \times l_y = 414 \times 314$ mm^2 and thickness 1 mm which is mounted on a rectangular cavity of dimensions $l_{xb} \times l_{yb} \times l_{zb} = 414 \times 314 \times 385$ mm^3. The panel is either excited by a transverse point force, acting at position x_f, $y_f = 120, 86$ mm or by the acoustic field generated in the cavity by a monopole source which is positioned at x_p, y_p, $z_p = 200, 120, 5$ mm.

As shown in Fig. 2, the panel is equipped with an array of 4×4 control systems that operate independently. The 16 control systems have been equally spaced along the x- and y-directions so that the distances between two actuators or between a lateral actuator and the edge of the plate are $d_x = l_x/5 = 82.8$ mm and $d_y = l_y/5 = 62.8$ mm. Each control system consists of a piezoceramic actuator, of dimensions $a_x \times a_y \times h_p = 25$ mm $\times$ 25 mm $\times$ 0.5 mm, which is bonded on the excited side of the panel and a small accelerometer placed on the other side of the panel in correspondence with the centre of the actuator. The actuator is driven by a single-channel analogue controller that implements velocity feedback control. Tables 1 and 2 summarize the assumed geometrical and physical properties of the smart panel and piezoceramic actuators.

4. Mathematical model

A fully coupled model is used to describe the effects of the acoustic cavity on the dynamics of the panel. In contrast, it is assumed that the acoustic pressure of the radiated sound has no effect

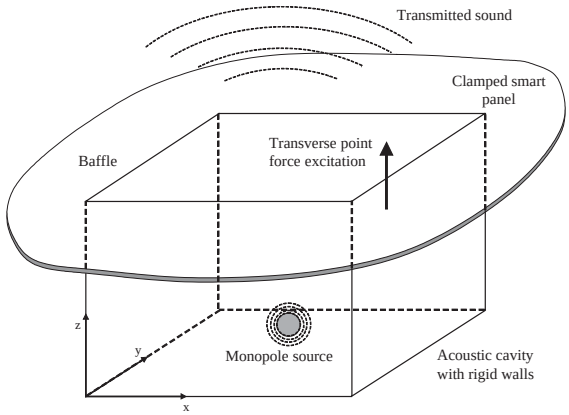

Fig. 1. Physical arrangement for the computer simulations, in which the vibration of a baffled clamped panel is excited either by the sound field in the cavity underneath it generated by a monopole source or by a transverse point force and radiates sound into an anechoic half-space on the other side of the panel.

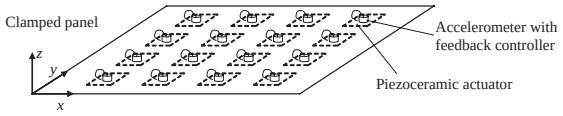

Fig. 2. Smart panel with a 4×4 array of decentralized control systems composed by an accelerometer sensor with a built in feedback control system and a piezoceramic actuator.

Table 1
Geometry and physical constants for the panel

Parameter	Value
Dimensions	$l_x \times l_y = 414 \times 314$ mm^2
Thickness	$h_s = 1$ mm
Mass density	$\rho_s = 2700$ kg/m^3
Young's modulus	$E_s = 7 \times 10^{10}$ N/m^2
Poisson ratio	$v_s = 0.33$
Loss factor	$\eta_s = 0.05$
Smeared mass density	$\bar{\rho}_s = 3000$ kg/m^3
Smeared Young's modulus	$\bar{E}_s = 7.1 \times 10^{10}$ N/m^2

Table 2
Geometry and physical constants for the piezoceramic, PZT, patches

Parameter	Value
Dimensions of the PZT patches	$a_x \times a_y = 25 \times 25$ mm^2
Thickness of the PZT patches	$h_p = 0.5$ mm
Young's modulus	$E_p = 2 \times 10^9$ N/m^2
Poisson ratio	$v_p = 0.29$
Stress constant	$e_{31} = 0.052$ N/V m
Strain constant	$d_{31} = 23 \times 10^{-12}$ m/V
Distance between the centres of two patches	d_x, $d_y = 82.8$, 62.8 mm

on the vibration of the panel, which is a reasonable assumption for air and this thickness of panel. The steady state response of the panel and sound radiation in a frequency range 0–2 kHz have been calculated assuming the primary disturbance acting on the panel or in the cavity to be harmonic with time dependence of the form $\mathrm{Re}\{\exp(\mathrm{j}\omega t)\}$. The velocity- and force-type parameters used in the model have been taken to be the real part of counterclockwise rotating complex vectors, so that: $\dot{w}(t) = \mathrm{Re}\{\dot{w}(\omega)\mathrm{e}^{\mathrm{j}\omega t}\}$ or $f(t) = \mathrm{Re}\{f(\omega)\mathrm{e}^{\mathrm{j}\omega t}\}$ where $\dot{w}(\omega)$ and $f(\omega)$ are the velocity and force phasors at $t = 0$, ω is the circular frequency and $\mathrm{j} = \sqrt{-1}$.

As shown in Fig. 3, the mathematical model built in for the simulations considers the panel divided into a grid of rectangular elements whose dimensions have been taken to be $l_{xe} = l_x/(4M)$ and $l_{ye} = l_y/(4N)$, where M and N are the higher plate modal orders used in the calculus. The top side of the cavity is also divided into a grid of rectangular elements of equal dimensions to those defined for the panel as shown in Fig. 3.

The phasors of the transverse velocities and forces, $\dot{w}_j(\omega)$ and $f_{zj}(\omega)$, at the centres of the panel and cavity elements have been, respectively, grouped into the following vectors:

$$\mathbf{v}_e(\omega) \equiv \begin{Bmatrix} \dot{w}_{e1}(\omega) \\ \dot{w}_{e2}(\omega) \\ \vdots \\ \dot{w}_{eP}(\omega) \end{Bmatrix}, \quad \mathbf{f}_e(\omega) \equiv \begin{Bmatrix} f_{ze1}(\omega) \\ f_{ze2}(\omega) \\ \vdots \\ f_{zeP}(\omega) \end{Bmatrix}$$

and

$$\mathbf{v}_b(\omega) \equiv \begin{Bmatrix} \dot{w}_{b1}(\omega) \\ \dot{w}_{b2}(\omega) \\ \vdots \\ \dot{w}_{bP}(\omega) \end{Bmatrix}, \quad \mathbf{f}_b(\omega) \equiv \begin{Bmatrix} f_{zb1}(\omega) \\ f_{zb2}(\omega) \\ \vdots \\ f_{zbP}(\omega) \end{Bmatrix}, \tag{1–4}$$

where $P = 16MN$ is the total number of elements. Similarly the phasors of the transverse velocities, $\dot{w}_{ci}(\omega)$, and forces, $f_{zci}(\omega)$, acting on the centres of each control unit have been defined as follows:

$$\mathbf{v}_c(\omega) \equiv \begin{Bmatrix} \dot{w}_{c1}(\omega) \\ \dot{w}_{c2}(\omega) \\ \vdots \\ \dot{w}_{c16}(\omega) \end{Bmatrix}, \quad \mathbf{f}_c(\omega) \equiv \begin{Bmatrix} f_{zc1}(\omega) \\ f_{zc2}(\omega) \\ \vdots \\ f_{zc16}(\omega) \end{Bmatrix}. \tag{5, 6}$$

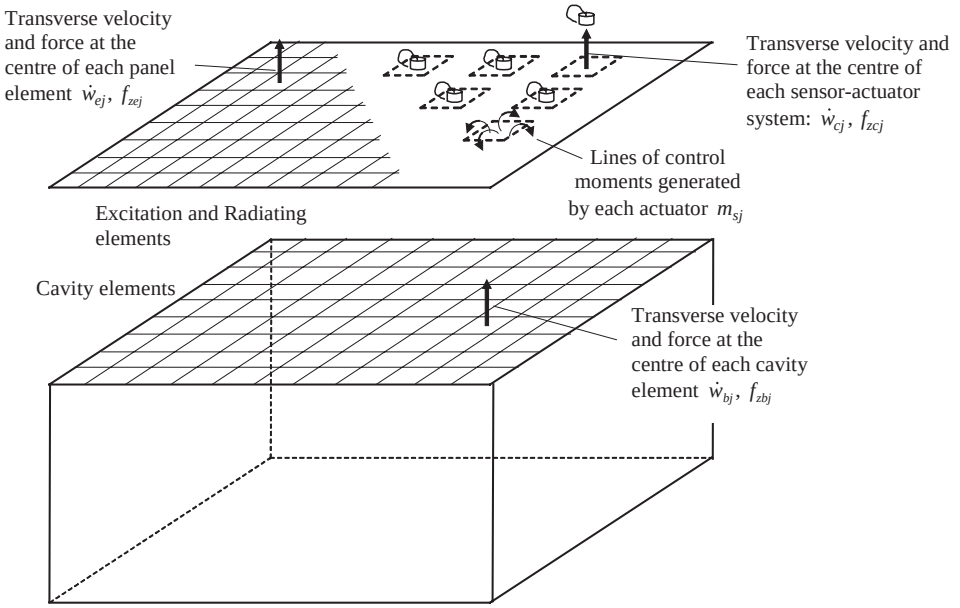

Fig. 3. Velocity and force-moment notation used in the mathematical model.

The primary excitations are given either by the amplitude of the transverse force acting on the panel or by the strength of the monopole acoustic source placed in the cavity which have been grouped in the two excitation vectors below, respectively:

$$\mathbf{f}_p(\omega) = f_p(\omega)\mathrm{e}^{\mathrm{j}\omega t}, \quad \mathbf{q}_p(\omega) = q_p(\omega)\mathrm{e}^{\mathrm{j}\omega t}. \tag{7,8}$$

The excitations of the 16 piezoceramic control actuators can be approximated by four line moments, all with equal magnitude, acting along the edges of the piezoceramic patches so that the control excitations can be grouped into a vector of moments as follows:

$$\mathbf{f}_s(\omega) = \begin{Bmatrix} m_{s1}(\omega) \\ m_{s2}(\omega) \\ \vdots \\ m_{s16}(\omega) \end{Bmatrix}. \tag{9}$$

The vibration of the panel at the centres of the elements and at the centres of the control systems can be expressed in matrix form using mobility functions so that

$$\mathbf{v}_e(\omega) = \mathbf{Y}_{ec}(\omega)\mathbf{f}_c(\omega) + \mathbf{Y}_{ee}(\omega)\mathbf{f}_e(\omega) + \mathbf{Y}_{ep}(\omega)\mathbf{f}_p(\omega) + \mathbf{Y}_{es}(\omega)\mathbf{f}_s(\omega), \tag{10}$$

$$\mathbf{v}_c(\omega) = \mathbf{Y}_{cc}(\omega)\mathbf{f}_c(\omega) + \mathbf{Y}_{ce}(\omega)\mathbf{f}_e(\omega) + \mathbf{Y}_{cp}(\omega)\mathbf{f}_p(\omega) + \mathbf{Y}_{cs}(\omega)\mathbf{f}_s(\omega), \tag{11}$$

where the components of the velocity/force mobility matrices, $\mathbf{Y}_{ec}(\omega)$, $\mathbf{Y}_{ee}(\omega)$, $\mathbf{Y}_{ep}(\omega)$ and $\mathbf{Y}_{cc}(\omega)$, $\mathbf{Y}_{ce}(\omega)$, $\mathbf{Y}_{cp}(\omega)$, between the positions $i = (x_i, y_i)$ and $k = (x_k, y_k)$, are given by [102]

$$Y^{i,k}(\omega) = \frac{\dot{w}_i(\omega)}{f_{z,k}(\omega)} = \mathrm{j}\omega \sum_{m=1}^{M} \sum_{n=1}^{N} \frac{\phi_{mn}(x_i, y_i)\phi_{mn}(x_k, y_k)}{\Lambda_{mn}[\omega_{mn}^2(1 + \mathrm{j}\eta_s) - \omega^2]} \tag{12}$$

and the components of the velocity/piezoceramic pact excitation matrices, $\mathbf{Y}_{es}(\omega)$ and $\mathbf{Y}_{cs}(\omega)$, between the position $i = (x_i, y_i)$ and the piezoceramic patch actuator position $k = (x_k, y_k)$, are given by

$$Y^{i,k}(\omega) = \frac{\dot{w}_i(\omega)}{m_k(\omega)} = \mathrm{j}\omega \sum_{m=1}^{M} \sum_{n=1}^{N} \times \frac{\phi(x_i, y_i)\{\int_0^{a_x}(\psi_{mn}^y(x_k, y_{k1}) - \psi_{mn}^y(x_k, y_{k2}))\,\mathrm{d}x_k + \int_0^{a_y}(-\psi_{mn}^x(x_{k1}, y_k) + \psi_{mn}^x(x_{k2}, y_k))\,\mathrm{d}y_k\}}{\Lambda_{mn}[\omega_{mn}^2(1 + \mathrm{j}\eta_s) - \omega^2]}, \tag{13}$$

where

m, n	the modal indices
ω_{mn}	the natural frequency of the (m, n)th bending mode
$\phi_{mn}(x, y)$	the (m, n)th bending natural mode at position (x, y)
Λ_{mn}	the modal normalization parameter $(= \rho_s h_s l_x l_y/4)$
ρ_s	the density of the material of the panel
h_s	the thickness of the panel
η_s	the hysteresis loss factor
$\psi_{mn}^x(x, y)$	the first derivative in x direction of $\phi_{mn}(x, y)$ $(= -\partial\phi_{mn}(x, y)/\partial x)$

$\psi^y_{mn}(x,y)$ the first derivative in y direction of $\phi_{mn}(x,y)$ $(= \partial\phi_{mn}(x,y)/\partial y)$
a_x, a_y the dimensions of the piezoceramic patch
x_{k1}, x_{k2} the x-positions of the two a_y edges of the kth piezoceramic patch
y_{k1}, y_{k2} the y-positions of the two a_x edges of the kth piezoceramic patch

The natural frequencies and natural modes of the clamped panel have been calculated using the formulation presented in Ref. [103].

The vector with the phasors of the transverse forces, f_{zbi}, acting at the centres of the elements on the top side of the box is given by

$$\mathbf{f}_b(\omega) = \mathbf{Z}_{bb}(\omega)\mathbf{v}_b(\omega) + \mathbf{Z}_{bq}(\omega)\mathbf{q}_p(\omega), \tag{14}$$

where assuming the area of the elements to be small compared to the bending and acoustic wavelengths in the frequency range considered in the simulations presented in this paper, the elements of the force/velocity impedance matrices between the positions $i = (x_i, y_i, l_{zb})$ and $k = (x_k, y_k, l_{zb})$ are given by

$$Z^{i,k}_{bb}(\omega) = \frac{f_{z,i}(\omega)}{\dot{w}_k(\omega)} = \sum_{r=1}^{R}\sum_{s=1}^{S}\sum_{t=1}^{T} \frac{\omega\rho_o c_o^2 \Delta S^2 \chi_{rst}(x_i, y_i, l_{zb})\chi_{rst}(x_k, y_k, l_{zb})}{\Lambda_{rst}[2\zeta_{rst}\omega_{rst}\omega + \mathrm{j}(\omega^2 - \omega^2_{rst})]}, \tag{15}$$

and the elements of the velocity/primary-excitation impedance matrix between the positions $i = (x_i, y_i, l_{zb})$ and the position $p = (x_p, y_p, z_p)$ of the monopole source are given by

$$Z^{i,p}_{bp}(\omega) = \frac{f_{z,i}(\omega)}{q_p(\omega)} = \sum_{r=1}^{R}\sum_{s=1}^{S}\sum_{t=1}^{T} \frac{\omega\rho_o c_o^2 \Delta S \chi_{rst}(x_i, y_i, l_{zb})\chi_{rst}(x_p, y_p, z_p)}{\Lambda_{rst}[2\zeta_{rst}\omega_{rst}\omega + \mathrm{j}(\omega^2 - \omega^2_{rst})]}, \tag{16}$$

where

r, s, t the modal indices
ω_{rst} the natural frequency of the (r, s, t)th mode
$\chi_{rst}(x, y, z)$ the (r, s, t)th cavity natural mode at position (x, y, z)
c_o the speed of sound
ρ_o the density of air
ζ_{rst} the damping ratio or the (r, s, t)th mode
ΔS the area of the elements
Λ_{rst} the modal normalization parameter $(= l_{xb} l_{yb} l_{zb})$

The natural frequencies and natural modes of the rectangular cavity have been calculated using the formulation presented in Ref. [104].

The panel is equipped with 16 control units, thus their dynamics effects should be taken into account even at low frequencies. Since the piezoceramic patches are evenly distributed over the panel surface and, up to 2 kHz, their surface dimensions are negligible compared to the wavelength of the bending vibration in the panel, then their stiffness and part of the mass effects can be modelled as a smeared effect over the entire surface of the panel so that low order mode shapes remain unaltered and the variation of the natural frequencies can be easily derived assuming a higher bending stiffness and density of the panel. The local dynamics of sensor–accelerometer plus part of the mass effect of the piezoceramic actuator have instead been

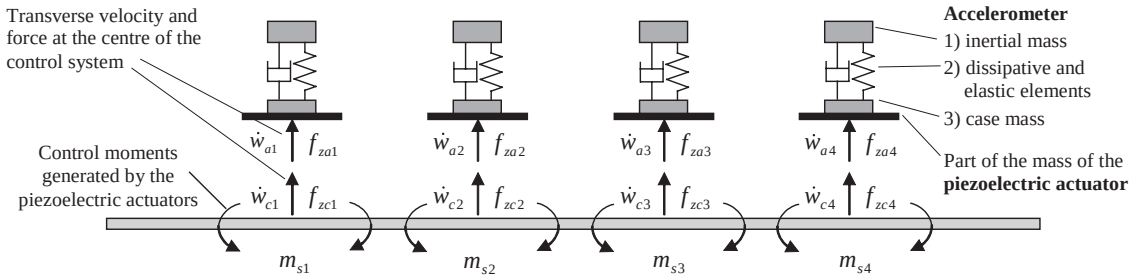

Fig. 4. Schematic representation of the sensor–actuator elements, which are represented by four lumped elements: the mass of the piezoceramic actuator, the mass of the case of the accelerometer and the spring and inertial mass of the accelerometer.

considered with a lumped parameter model that accounts for the inertial mass, m_a, stiffness and damping of the accelerometer, k_a and c_a, and the mass of accelerometer case plus part of the mass of the piezoceramic actuator, m_{ac} and m_p, arranged as shown in Fig. 4. The phasors of the transverse velocities, $\dot{w}_{aj}(\omega)$, and forces, $f_{zaj}(\omega)$, at the centres of each control systems can be related by the following impedance expression:

$$f_{zaj}(\omega) = Z_{eq}(\omega)\dot{w}_{aj}(\omega), \tag{17}$$

where the driving point impedance of each accelerometer sensor $Z_{eq}(\omega)$ has been derived in Ref. [105] to be

$$Z_{eq}(\omega) = \frac{f_a(\omega)}{\dot{w}_a(\omega)} = \frac{1 - T(\omega)}{Y_1(\omega)}, \tag{18}$$

where

$$T(\omega) = -Y_1(\omega)Z_{m11}(\omega) + \frac{Y_1(\omega)Z_{m12}(\omega)\,Y_2(\omega)Z_{m21}(\omega)}{1 + Y_2(\omega)Z_{m22}(\omega)} \tag{19}$$

and

$$Y_2(\omega) = \frac{1}{\mathrm{j}\omega m_a}, \quad Y_1(\omega) = \frac{1}{\mathrm{j}\omega m_{ac}}, \tag{20a, b}$$

$$Z_{m11}(\omega) = \left(c_a + \frac{k_a}{\mathrm{j}\omega}\right), \quad Z_{m12}(\omega) = -\left(c_a + \frac{k_a}{\mathrm{j}\omega}\right),$$
$$Z_{m21}(\omega) = -\left(c_a + \frac{k_a}{\mathrm{j}\omega}\right), \quad Z_{m22}(\omega) = \left(c_a + \frac{k_a}{\mathrm{j}\omega}\right). \tag{21a–d}$$

In the simulations the physical parameters given in Table 3 have been used. As discussed above the mass effect of the piezoceramic actuators has been taken into account partially as a localized effect and partially as a smeared effect over the panel surface. As a result, the lumped mass of each piezoceramic actuator has been taken to be $m_p = 0.2 \times 10^{-3}$ kg, although the true mass is 1×10^{-3} kg. In order to account for the smeared inertia effect of the 16 piezoceramic actuators, the density of the material of the panel has been taken to be $\bar{\rho}_s = 3000\ \mathrm{kg/m^3}$. The stiffening effect of the piezoceramic actuators has also been smeared over the panel and thus Young's modulus of elasticity used in the simulations has been assumed to be $\bar{E}_s = 7.1 \times 10^{10}\ \mathrm{N/m^2}$.

Table 3
Physical properties of the sensor and actuator

Parameter	Value
Mass of the piezoceramic actuator	$m_p = 0.2 \times 10^{-3}$ kg
Mass of the accelerometer case	$m_{ac} = 0.2 \times 10^{-3}$ kg
Inertia mass of the accelerometer	$m_a = 0.22 \times 10^{-3}$ kg
Internal stiffness of the accelerometer	$k_a = 1.1 \times 10^7$ N/m
Mounted frequency resonance of accelerometer	$f_a = \omega_n/2\pi = 33.6 \times 10^3$ Hz
Damping coefficient of the accelerometer	$c_a = 2.5$ N/ms

Defining the vectors $\mathbf{v}_a(\omega)$ and $\mathbf{f}_a(\omega)$ to be given by the velocities and forces at the bottom of the accelerometer sensors, respectively:

$$\mathbf{v}_a(\omega) \equiv \begin{Bmatrix} \dot{w}_{a1}(\omega) \\ \dot{w}_{a2}(\omega) \\ \vdots \\ \dot{w}_{a16}(\omega) \end{Bmatrix}, \quad \mathbf{f}_a(\omega) \equiv \begin{Bmatrix} f_{za1}(\omega) \\ f_{za2}(\omega) \\ \vdots \\ f_{za16}(\omega) \end{Bmatrix}, \tag{22, 23}$$

then

$$\mathbf{f}_a(\omega) = \mathbf{Z}_{aa}(\omega)\mathbf{v}_a(\omega), \tag{24}$$

where the impedance matrix $\mathbf{Z}_{aa}(\omega)$ is diagonal

$$\mathbf{Z}_{aa}(\omega) = \begin{bmatrix} Z_{eq1} & & & \\ & Z_{eq2} & & \\ & & \ddots & \\ & & & Z_{eq16} \end{bmatrix}. \tag{25}$$

The response of the panel taking into account the coupled response with the acoustic cavity and with the dynamics of the 16 control units can now be derived using the dynamic equilibrium and compatibility principles at the connecting points between the centres of the elements of the panel and those of the acoustic cavity and at the connecting points between the 16 control positions in the panel and the centres of 16 control units so that:

	Elements centres	*Control points*	
(a) dynamic equilibrium	$\mathbf{f}_e + \mathbf{f}_b = \mathbf{0}$	$\mathbf{f}_c + \mathbf{f}_a = \mathbf{0}$	(26)
(b) compatibility	$\mathbf{v}_e = \mathbf{v}_b$	$\mathbf{v}_c = \mathbf{v}_a$	(27)

Using Eqs. (10), (11), (14) and (24) the following two relations can be derived for the velocities of the panel at the element centres and at the control points:

$$\mathbf{v}_e(\omega) = -\mathbf{Q}_{ec}(\omega)\mathbf{v}_c(\omega) - \mathbf{Q}_{eq}(\omega)\mathbf{q}_p(\omega) + \mathbf{Q}_{ep}(\omega)\mathbf{f}_p(\omega) + \mathbf{Q}_{es}(\omega)\mathbf{f}_s(\omega), \tag{28}$$

$$\mathbf{v}_c(\omega) = -\mathbf{Q}_{ce}(\omega)\mathbf{v}_e(\omega) - \mathbf{Q}_{cq}(\omega)\mathbf{q}_p(\omega) + \mathbf{Q}_{cp}(\omega)\mathbf{f}_p + \mathbf{Q}_{cs}(\omega)\mathbf{f}_s(\omega), \tag{29}$$

where

$$\mathbf{Q}_{ec}(\omega) = (\mathbf{I} + \mathbf{Y}_{ee}\mathbf{Z}_{bb})^{-1}\mathbf{Y}_{ec}\mathbf{Z}_{aa}, \quad \mathbf{Q}_{ce}(\omega) = (\mathbf{I} + \mathbf{Y}_{cc}\mathbf{Z}_{aa})^{-1}\mathbf{Y}_{ce}\mathbf{Z}_{bb},$$
$$\mathbf{Q}_{eq}(\omega) = (\mathbf{I} + \mathbf{Y}_{ee}\mathbf{Z}_{bb})^{-1}\mathbf{Y}_{ee}\mathbf{Z}_{bq}, \quad \mathbf{Q}_{cq}(\omega) = (\mathbf{I} + \mathbf{Y}_{cc}\mathbf{Z}_{aa})^{-1}\mathbf{Y}_{ce}\mathbf{Z}_{bq},$$
$$\mathbf{Q}_{ep}(\omega) = (\mathbf{I} + \mathbf{Y}_{ee}\mathbf{Z}_{bb})^{-1}\mathbf{Y}_{ep}, \quad \mathbf{Q}_{cp}(\omega) = (\mathbf{I} + \mathbf{Y}_{cc}\mathbf{Z}_{aa})^{-1}\mathbf{Y}_{cp},$$
$$\mathbf{Q}_{es}(\omega) = (\mathbf{I} + \mathbf{Y}_{ee}\mathbf{Z}_{bb})^{-1}\mathbf{Y}_{es}, \quad \mathbf{Q}_{cs}(\omega) = (\mathbf{I} + \mathbf{Y}_{cc}\mathbf{Z}_{aa})^{-1}\mathbf{Y}_{cs}, \tag{30a–h}$$

where $\mathbf{I}$ is the unit matrix. Eqs. (28) and (29) can further be manipulated to get

$$\mathbf{v}_e(\omega) = \mathbf{T}_{eq}(\omega)\mathbf{q}_p(\omega) - \mathbf{T}_{ep}(\omega)\mathbf{f}_p(\omega) - \mathbf{T}_{es}(\omega)\mathbf{f}_s(\omega), \tag{31}$$

$$\mathbf{v}_c(\omega) = \mathbf{T}_{cq}(\omega)\mathbf{q}_p(\omega) - \mathbf{T}_{cp}(\omega)\mathbf{f}_p(\omega) - \mathbf{T}_{cs}(\omega)\mathbf{f}_s(\omega), \tag{32}$$

where

$$\mathbf{T}_{eq}(\omega) = (\mathbf{I} - \mathbf{Q}_{ec}\mathbf{Q}_{ce})^{-1}(\mathbf{Q}_{ec}\mathbf{Q}_{cq} - \mathbf{Q}_{eq}), \quad \mathbf{T}_{cq}(\omega) = (\mathbf{I} - \mathbf{Q}_{ce}\mathbf{Q}_{ec})^{-1}(\mathbf{Q}_{ce}\mathbf{Q}_{eq} - \mathbf{Q}_{cq}),$$
$$\mathbf{T}_{ep}(\omega) = (\mathbf{I} - \mathbf{Q}_{ec}\mathbf{Q}_{ce})^{-1}(\mathbf{Q}_{ec}\mathbf{Q}_{cp} - \mathbf{Q}_{ep}), \quad \mathbf{T}_{cp}(\omega) = (\mathbf{I} - \mathbf{Q}_{ce}\mathbf{Q}_{ec})^{-1}(\mathbf{Q}_{ce}\mathbf{Q}_{ep} - \mathbf{Q}_{cp}),$$
$$\mathbf{T}_{es}(\omega) = (\mathbf{I} - \mathbf{Q}_{ec}\mathbf{Q}_{ce})^{-1}(\mathbf{Q}_{ec}\mathbf{Q}_{cs} - \mathbf{Q}_{es}), \quad \mathbf{T}_{cs}(\omega) = (\mathbf{I} - \mathbf{Q}_{ce}\mathbf{Q}_{ec})^{-1}(\mathbf{Q}_{ce}\mathbf{Q}_{es} - \mathbf{Q}_{cs}), \tag{33a–f}$$

where $\mathbf{I}$ is the unit matrix. The accelerometer sensor operates as a single degree resonant system with relatively high-natural frequency, in general about 30–50 kHz, and thus the high-frequency response of the panel with the 16 accelerometer sensors could be quite different to that of the panel on itself. The output signal of accelerometers is proportional to the differential acceleration of the accelerometer—mass and accelerometer—case so that, for a given velocity at the mounting point of the accelerometer $\dot{w}_c = \dot{w}_a$, the measured value is given by

$$\dot{w}_{\mathrm{mes}}(\omega) = A(\omega)\dot{w}_c(\omega), \tag{34}$$

where $A(\omega)$ is the accelerometer frequency response function [106]:

$$A(\omega) = \frac{m_a}{k_a - m_a\omega^2 + \mathrm{j}c_a\omega} = \frac{1}{\omega_n^2 - \omega^2 + \mathrm{j}\xi_a 2\omega\omega_n}, \tag{35}$$

where $\omega_n = \sqrt{k_a/m_a}$ is the accelerometer natural frequency and $\xi_a = c_a/2\sqrt{k_a m_a}$ is the damping ratio of the accelerometer.

The measured velocities by the 16 accelerometers can be grouped in the following vector:

$$\mathbf{v}_m(\omega) \equiv \begin{Bmatrix} \dot{w}_{m1}(\omega) \\ \dot{w}_{m2}(\omega) \\ \vdots \\ \dot{w}_{m16}(\omega) \end{Bmatrix}, \tag{36}$$

which can be related to the panel velocities at the control points by the following matrix relation:

$$\mathbf{v}_m(\omega) = \mathbf{A}(\omega)\mathbf{v}_c(\omega), \tag{37}$$

where

$$\mathbf{A}(\omega) = \begin{bmatrix} A_1 & & & \\ & A_2 & & \\ & & \ddots & \\ & & & A_{16} \end{bmatrix}. \tag{38}$$

When there is no control action, i.e., $\mathbf{f}_s(\omega) \equiv \mathbf{0}$, then the transverse velocities at the centre positions of the elements of the panel can be calculated directly from Eq. (31) to be

$$\mathbf{v}_e(\omega) = \mathbf{T}_{eq}(\omega)\mathbf{q}_p(\omega) - \mathbf{T}_{ep}(\omega)\mathbf{f}_p(\omega), \tag{39}$$

Provided the control system is stable, if, as shown in Fig. 5, for each sensor–actuator pair a decentralized feedback control loop is implemented with constant velocity feedback gain, h, such that

$$\mathbf{f}_s(\omega) = -\mathbf{H}(\omega)\mathbf{v}_m(\omega). \tag{40}$$

where

$$\mathbf{H}(\omega) = \begin{bmatrix} h_1 & & & \\ & h_2 & & \\ & & \ddots & \\ & & & h_{16} \end{bmatrix}, \tag{41}$$

then, as can be deduced by the block diagram in Fig. 5, the velocities at the accelerometer positions given by Eq. (32) are found to be

$$\mathbf{v}_c(\omega) = (\mathbf{I} - \mathbf{T}_{cs}(\omega)\mathbf{H}\mathbf{A}(\omega))^{-1}\{\mathbf{T}_{cq}(\omega)\mathbf{q}_p(\omega) - \mathbf{T}_{cp}(\omega)\mathbf{f}_p(\omega)\} \tag{42}$$

and the transverse velocities at the centre positions of the elements of the panel given by Eq. (31) are given by

$$\begin{aligned}\mathbf{v}_e(\omega) = {} & \mathbf{T}_{eq}(\omega)\mathbf{q}_p(\omega) - \mathbf{T}_{ep}(\omega)\mathbf{f}_p(\omega) \\ & + \mathbf{T}_{es}(\omega)\mathbf{H}\mathbf{A}(\omega)(\mathbf{I} - \mathbf{T}_{cs}(\omega)\mathbf{H}\mathbf{A}(\omega))^{-1}\{\mathbf{T}_{cq}(\omega)\mathbf{q}_p(\omega) - \mathbf{T}_{cp}(\omega)\mathbf{f}_p(\omega)\}.\end{aligned} \tag{43}$$

It should be underlined that these results are valid provided the 16 decentralized feedback control units are all stable. Elliott et al. [3] have shown that this is true when collocated and compatible transducers are used. These authors have also shown that for a velocity sensor and a collocated

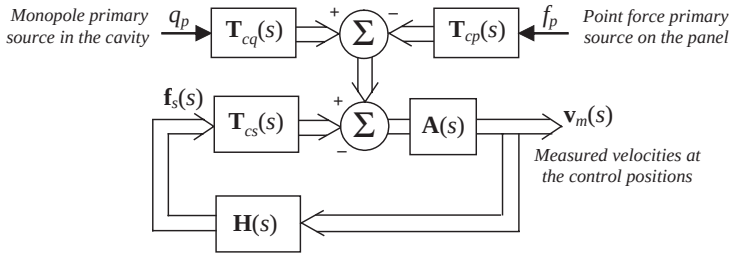

Fig. 5. Block diagram of the decentralized feedback control system implemented in the smart panel, $s = j\omega$.

piezoceramic actuator patch, where the actuator is modelled as a set of four line-moment excitations, the plant response is positive real at low frequencies and so a feedback control system would be stable. In the second part of this paper the true behaviour of these two transducers is analyzed in more detail both experimentally and numerically. It is shown that when the true transducers are analyzed, each control unit is not guaranteed to be stable above few kilohertz. Only a limited feedback gain can thus be used in Eqs. (42) and (43).

The total kinetic energy of the panel or the total sound power radiated per unit primary excitation can be derived from the velocities of the radiating elements given in Eqs. (39) and (43). The total kinetic energy of the panel is given by

$$E(\omega) = \frac{\rho_s h_s}{4} \int_0^{l_x} \int_0^{l_y} |\dot{w}(x, y, \omega)|^2 \, \mathrm{d}x \, \mathrm{d}y. \tag{44}$$

This expression can be approximated to the summation of the kinetic energies of each element into which the panel has been subdivided so that

$$E(\omega) = \frac{m_s}{4} \mathbf{v}_e^{\mathrm{H}}(\omega) \mathbf{v}_e(\omega), \tag{45}$$

where $m_s = \rho_s h_s l_{xe} l_{ye}$ is the mass of the elements and H denotes the Hermitian transpose. The total sound power radiation by a baffled panel can be derived by integrating the product of the near-field sound pressure on the radiating side and the transverse velocity of the panel so that

$$W(\omega) = \frac{1}{2} \int_0^{l_x} \int_0^{l_y} p_o(x, y, \omega)^* \dot{w}(x, y, \omega) \, \mathrm{d}x \, \mathrm{d}y, \tag{46}$$

where $*$ denotes the complex conjugate. The sound pressure in front of the panel $p(x, y, \omega)$ is related to the transverse velocity of the panel at the same position $\dot{w}(x, y, \omega)$ by the specific acoustic impedance in air Z_o so that

$$p(x, y, \omega) = Z_o(x, y, \omega) \dot{w}(x, y, \omega). \tag{47}$$

Similarly to the case of kinetic energy, the integral in Eq. (46) can be approximated to the radiated sound power by all the elements into which the panel has been subdivided so that the total sound power radiation can be expressed as

$$W(\omega) = \frac{\Delta S}{2} \mathrm{Re}[\mathbf{v}_e^{\mathrm{H}}(\omega) \mathbf{p}(\omega)], \tag{48}$$

where $\mathbf{p}(\omega)$ is the vector with the phasors of the sound pressure in front of the panel at the centre positions of the grid of elements:

$$\mathbf{p}(\omega) = \begin{Bmatrix} p_1(\omega) \\ p_2(\omega) \\ \vdots \\ p_{16}(\omega) \end{Bmatrix}. \tag{49}$$

Eq. (48) can also be written as

$$W(\omega) = \frac{\Delta S}{2} \mathrm{Re}[\mathbf{v}_e^{\mathrm{H}}(\omega) \mathbf{Z}(\omega) \mathbf{v}_e(\omega)] = \mathbf{v}_e^{\mathrm{H}}(\omega) \mathbf{R}(\omega) \mathbf{v}_e(\omega), \tag{50}$$

where $\mathbf{Z}$ is the matrix with the point and transfer acoustic impedance terms over the grid of point into which the panel has been subdivided [32]

$$\mathbf{Z}(\omega) = \frac{\mathrm{j}\omega\rho_o \Delta S}{2\pi} \begin{bmatrix} 1 & \frac{\mathrm{e}^{-\mathrm{j}k_o r_{12}}}{r_{12}} & \cdots & \frac{\mathrm{e}^{-\mathrm{j}k_o r_{1I}}}{r_{1I}} \\ \frac{\mathrm{e}^{-\mathrm{j}k_o r_{21}}}{r_{21}} & 1 & & \\ \cdots & \cdots & \cdots & \cdots \\ \frac{\mathrm{e}^{-\mathrm{j}k_o r_{I1}}}{r_{I1}} & & & 1 \end{bmatrix}, \tag{51}$$

where $k_o = \omega/c_o$ is the acoustic wavenumber in air and r_{ij} is the distance between the ith and jth elements. The radiation matrix $\mathbf{R}$ is therefore given by [32]

$$\mathbf{R}(\omega) = \left(\frac{\Delta S}{2}\right) \mathrm{Re}[\mathbf{Z}(\omega)] = \frac{\omega^2 \rho_o \Delta S^2}{4\pi c_o} \begin{bmatrix} 1 & \frac{\sin(k_o r_{12})}{k_o r_{12}} & \cdots & \frac{\sin(k_o r_{1I})}{k_o r_{1I}} \\ \frac{\sin(k_o r_{21})}{k_o r_{21}} & 1 & & \\ \cdots & \cdots & \cdots & \cdots \\ \frac{\sin(k_o r_{I1})}{k_o r_{I1}} & & & 1 \end{bmatrix}. \tag{52}$$

Although the sound power radiated by the panel usefully quantifies the farfield pressure it generates, high vibration levels in weakly radiated modes can give rise to significant pressure levels in the near-field of the panel. It has been shown that the total kinetic energy of a panel provides a better measure of near-field pressure than radiated sound power [35], and so if there is any possibility that listeners may be in close proximity to the panel, as well as being further away, then both of these criteria are important for active structural acoustic control.

5. Simulations results

In this section the response of the panel and its sound radiation is discussed with reference to a range of feedback gains in the 16 decentralized control units. First, the analysis is carried out considering the system to be excited only by the monopole acoustic source placed within the cavity. The kinetic energy and sound power radiation, given by Eqs. (45) and (50), have been calculated using Eqs. (39) and (43) for the velocities of the radiating elements in the two cases of no control or active control.

Fig. 6 shows the total kinetic energy of the panel excited by the monopole acoustic source in the cavity when the 16 decentralized control units are implemented with various feedback gains, h. Since the primary excitation acts on the acoustic cavity, the low-frequency response of the panel before control is characterized by a selected number of panel or cavity natural frequencies. For example, the first three resonances are close to the natural frequencies of the panel relative to the modes (1,1), (1,3), and (3,1) which occur, respectively, at 69.7, 197.2 and 305.5 Hz and are well coupled to the low-frequency volumetric response of the cavity. The fourth resonance frequency

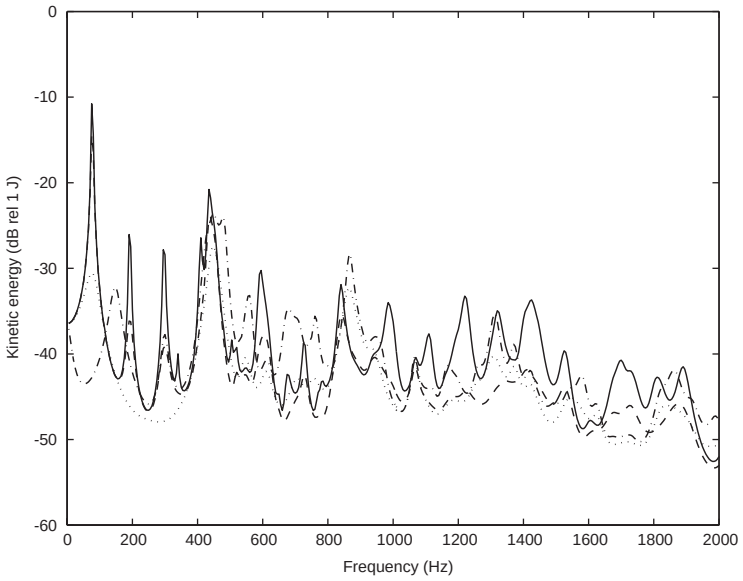

Fig. 6. Kinetic energy of the panel when it is excited by the acoustic monopole source. With no control, solid line, and with the 16 channel decentralized feedback control systems having a feedback gain of 10, dashed, 100, dotted, and 1000, dot–dashed lines.

shows a relatively high peak which is in fact due to the first two natural modes of the cavity, the (0,1,0) and the (0,0,1), which occur, respectively, at 414.3 and 445.5 Hz. These two cavity modes are well coupled to the panel modes (3,3) and (1,5) whose natural frequencies are at 420.8 and 441.1 Hz. At higher frequencies the same type of behaviour is seen where well-defined resonance peaks are found corresponding to either panel or cavity natural frequencies of strongly coupled panel-cavity modes. When the control system is turned on, it can be noticed that as the gains of the feedback loops are increased, the resonances which are controlled mainly by the panel natural modes become more heavily damped, as one would expect with velocity feedback control. In contrast, the resonances controlled by the cavity natural modes are not controlled. Also, it should be noted that the first resonance at 69.7 Hz which is controlled by the (1,1) mode of the panel requires much higher control gains to achieve the same control results obtained for higher order panel modes. This is probably due to the coupling of the (1,1) mode of the panel with the volumetric response of the cavity that produces a stiffening effect. Also, the piezoceramic patches are moment-type actuators that find difficulty in exciting bending of the panel at low frequencies [16]. If the gains of the feedback loops are increased beyond a certain value the closed-loop response displays new peaks, such as that at about 185 Hz for example, which becomes more pronounced as the feedback gain is increased. As discussed by Elliott et al. [3] these extra peaks are due to the resonances of the controlled panel, which is effectively pinned at the sensor positions with high feedback gains. If feedback controllers having very high gains were used, the velocities at each sensor could be driven to zero and thus the response of the panel would be characterized by a new set of natural modes defined by the clamping conditions at the four edges and by the pinning conditions at the 16 control points. It is important to underline that these new

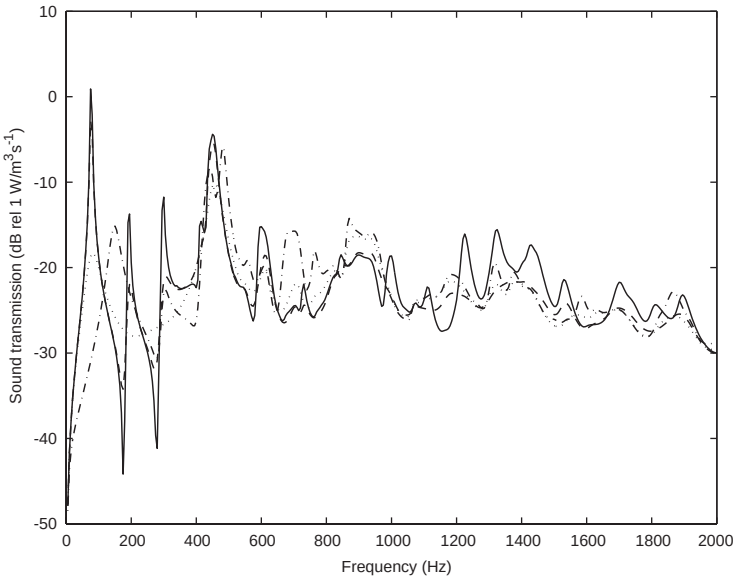

Fig. 7. Sound transmission of the panel when it is excited by the acoustic monopole source. With no control, solid line, and with the 16 channel decentralized control systems having a feedback gain of 10, dashed, 100, dotted, and 1000, dot–dashed lines.

modes are lightly damped since the 16 control units are not introducing any active damping effect having driven to zero the velocity at the control positions.

Fig. 7 shows the ratio of the sound power radiated on one side of the panel to the strength of the primary monopole source in the cavity which here is called sound transmission. As discussed above, before control, the response of the panel is controlled by the coupling of the panel-cavity modes. However, at low frequencies, only the panel modes whose modal integers are odd radiate sound significantly [21]. Also anti-resonances appear, due to destructive interference between the sound pressures radiated by adjacent odd modes [21]. As the feedback gains are increased, similar trends are observed in the reduction of the sound transmission coefficient as in the reduction of the kinetic energy of the panel, except that the new resonance at about 185 Hz has the greatest prominence, since its velocity distribution has the largest net volume velocity and therefore sound radiation. Also, it can be noticed that for those peaks controlled by cavity modes, for example those with natural frequencies 414.3 and 445.5 Hz, there is almost no reduction of the sound radiation for any value of the control gain. Indeed between 400 and 1200 Hz there is no control, on the contrary the sound radiation is enhanced for relatively high gains. Between 1200 and 1500 Hz good control levels are achieved despite the relatively higher frequencies.

When the kinetic energy of the panel is integrated across the bandwidth shown in Fig. 6 (up to 2 kHz) and this is plotted against feedback gain, a clear minimum of 7.4 dB is observed, for a gain of about 100, as shown in Fig. 8 (solid line). For higher gains the total kinetic energy after control is actually enhanced by about 2.8 dB because of the lightly damped new modal response of the panel as described above. The solid line in Fig. 9 shows the variation with feedback gain of the sound transmission ratio integrated across this bandwidth, which corresponds to the total

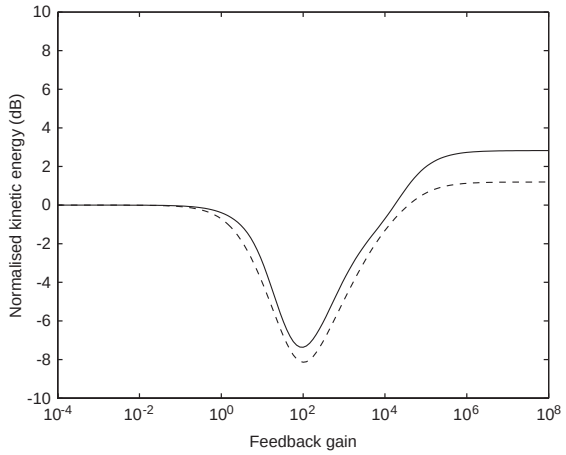

Fig. 8. Normalized kinetic energy level of the panel, integrated from 0 Hz to 2 kHz, plotted against the gain in the decentralized feedback controller, h, for the monopole acoustic primary source (solid line) and the force primary source (dashed line).

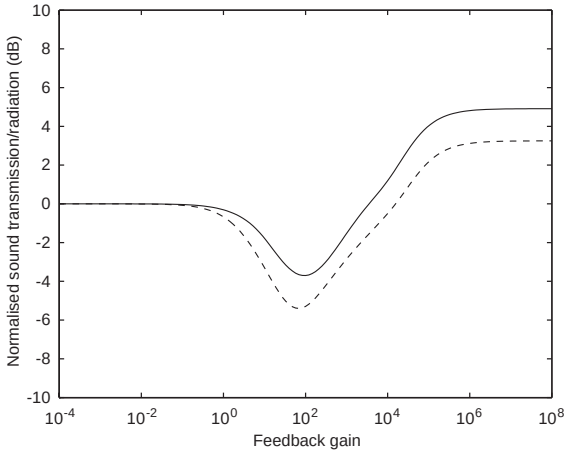

Fig. 9. Normalized sound transmission ratio, integrated from 0 Hz to 2 kHz, plotted against the gain in the decentralized feedback controller, h, for the monopole acoustic primary source (solid line) and the force primary source (dashed line).

radiated sound power if the plate is subject to broadband cavity excitation up to a frequency of 2 kHz, and this also has a minimum value of 3.7 dB for a feedback gain of about 100. At higher feedback gains the overall sound power radiated after control is some 4.8 dB higher than it was with no control, because of the lightly damped new modal response of the panel as described above.

The second analysis has been carried out considering the system to be excited only by the transverse point force acting on the panel. Fig. 10 shows the total kinetic energy of the panel before control and when subject to control with 16 decentralized control systems with various

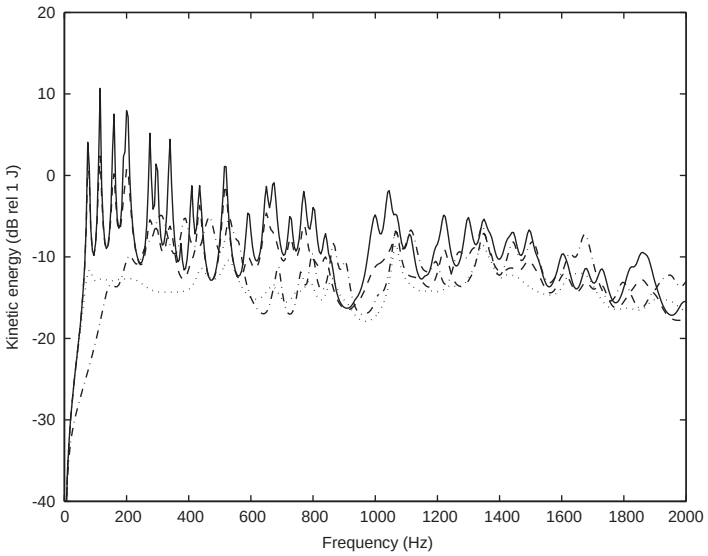

Fig. 10. Kinetic energy of the panel when it is excited by the force source. With no control, solid line, and with the 16 channel decentralized feedback control systems having a feedback gain of 10, dashed, 100, dotted, and 1000, dot–dashed lines.

feedback gains, h. The modal response of the panel is quite different to that shown in Fig. 6 since the point force excites most, if not all, the modes of the panel. Also, because the cavity exerts only a passive effect on the panel, then the cavity controlled peaky resonances seen in the previous analysis are not so marked in this case. Indeed at low frequencies the first four resonances are close to the first four natural frequencies of the panel modes (1,1), (1,2), (2,1) and (1,3) which occur at frequencies: 69.7, 117.9, 163.3 and 197.2 Hz. Also, there are not the dominant resonance peaks at about 414.3 and 445.5 Hz due to the cavity natural modes as found when the primary excitation is given by the monopole source in the cavity. In this case, when the control system is turned on, as the gains of the feedback loops are increased, most of the low-frequency resonances are progressively damped so that for an optimal gain of 100 an overall reduction of the kinetic energy of the panel of about 8.1 dB is achieved as shown by the dashed line in Fig. 8. For higher values of gains the response of the panel is characterized by a new set of resonance frequencies which, as seen above, are due to the new, lightly damped, modes of the panel generated by the control units which, for higher gains, are pinning the panel at the 16 control positions. As a result, for higher gains the overall kinetic energy in the frequency range 0–2 kHz is increased by about 1.2 dB as shown by the dashed line in Fig. 8. It is quite interesting to note also that in this case larger control gains are required to achieve the same level of control for the first few resonances of the panel as for the resonances at higher frequencies. As discussed above this is due to the coupling between the low-frequency natural modes and the volumetric response of the cavity which contrasts the action of the 16 control units. Fig. 11 shows the ratio of the sound power radiated on one side of the panel to the amplitude of the primary force acting on the panel. This spectrum is also characterized by a larger number of resonances when compared to that derived for the case in which the primary excitation is the monopole source in the cavity. Most of the resonances in the frequency range 0–2 kHz are damped when the optimal gain of about 100 is

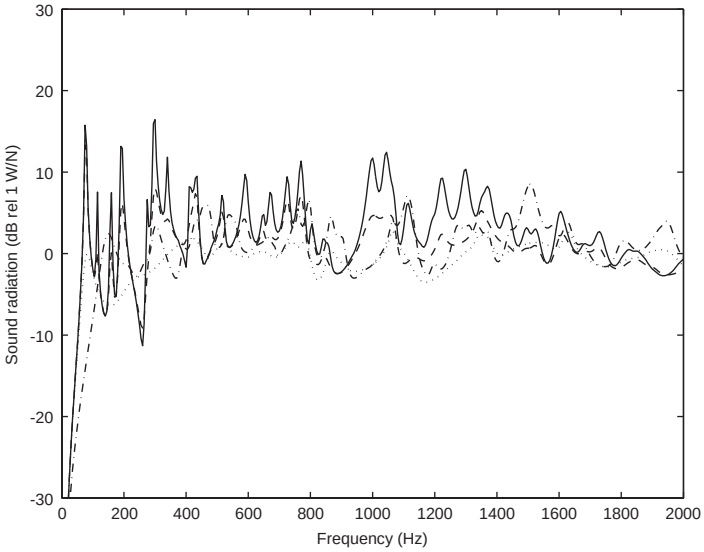

Fig. 11. Sound transmission of the panel when it is excited by the force source. With no control, solid line, and with the 16 channel decentralized feedback control systems having a feedback gain of 10, dashed, 100, dotted, and 1000, dot–dashed lines.

used so that an overall reduction of the sound radiation of about 5.5 dB is produced as shown by the dashed line in Fig. 9. Considering the optimal gain, some of the low-frequency modes of the panel are less damped because of the loading effect of the acoustic cavity. Also, as shown by the dashed line in Fig. 9, when higher values of gain are implemented, because of the pinning effect of the 16 control units, then the sound radiation is actually enhanced to about 3.2 dB.

6. Concluding remarks

This paper summarizes the theoretical work carried out to develop a prototype smart panel with 16 decentralized vibration control units which implement velocity feedback (i.e., active damping) for the reduction of sound radiation/transmission. The system studied consists of the clamped and baffled smart panel which is mounted on a rectangular cavity. The panel is excited either by a transverse point force or by the acoustic field generated in the cavity by a monopole source. The main conclusions of this study can be summarized in the following seven points:

1. The low-frequency response of the panel before control is characterized by a selected number of resonances that, in the case of the cavity primary source, correspond to either panel or cavity natural frequencies of well coupled panel-cavity modes and in the case of the force primary source, includes most, if not all, the modes of the panel.
2. At low-frequencies, only the modes whose modal integers are odd radiate sound significantly and also anti-resonances appear, due to destructive interference between the sound pressures radiated by adjacent odd modes.

3. When the control system is turned on, it can be noticed that as the gains of the feedback loops are increased, the resonances that are controlled mainly by the panel natural modes become more heavily damped. In contrast, the resonances controlled by the cavity natural modes are not damped.
4. Larger control gains are required to control the panel modes with natural frequencies below the first natural frequency of the cavity since the control units have to contrast the volumetric loading of the acoustic cavity on the panel.
5. When the system is excited by the monopole acoustic primary source in the cavity, it has been found that the kinetic energy or sound radiation integrated between 0 and 2 kHz are reduced, respectively, by 7.4 dB and 3.7 dB corresponding to the optimal gain of 100. For higher gains the control effectiveness degrades up to a point where the overall kinetic energy or sound radiation are enhanced by 2.8 and 4.8 dB, respectively.
6. Similar behaviour has been found when the system is excited by the primary force acting on the panel. For the optimal control gain of 100, the overall kinetic energy or sound radiation in the frequency range 0–2 kHz are reduced, respectively, by 8.1 and 5.5 dB while for higher gains there is an enhancement of 1.2 and 3.2 dB, respectively.
7. The degrading performance of the control systems when higher gains are used is due to the fact that, for very high control gains, each control unit pins the vibration at the control point so that the response of the panel is transformed to that of a lightly damped structure with a new set of natural modes having higher natural frequencies because of the new pinning boundary conditions corresponding to the 16 control systems.

A general review of the work done up to now to develop smart panels for the control of sound radiation/transmission has also been presented. In particular, the various stages that brought scientists to develop active structural acoustic control systems are discussed with reference to either feed-forward and feedback control approaches. The review highlights that for feed-forward control of tonal disturbances the sensor–actuator transducers must be designed to control radiation modes while for feedback active damping control of broadband random disturbances the sensor–actuator transducers should be designed to control structural modes.

Acknowledgements

The work carried out by Mr Bianchi for this study is within the ''European Doctorate in Sound and Vibration Studies'' which is supported through a European Community Marie Curie Fellowship.

References

[1] P. Gardonio, E. Bianchi, S.J. Elliott, Smart panel with multiple decentralized units for the control of sound transmission. Part II: design of the decentralized control units, *Journal of Sound and Vibration* 274 (1–2) (2004) 193–213, this issue.

[2] P. Gardonio, E. Bianchi, S.J. Elliott, Smart panel with multiple decentralized units for the control of sound transmission. Part III: control system implementation, *Journal of Sound and Vibration* 274 (1–2) (2004) 215–232, this issue.

[3] S.J. Elliott, P. Gardonio, T.J. Sors, M.J. Brennan, Active vibroacoustic control with multiple local feedback loops, *Journal of the Acoustical Society of America* 111 (2) (2002) 908–915.
[4] P.A. Nelson, S.J. Elliott, *Active Control of Sound*, 1st Edition, Academic Press, London, 1992.
[5] C.F. Ross, M.R. Purver, Active cabin noise control, *Proceedings of ACTIVE 97*, Budapest, Hungary, XXXIX-XLVI, 1997.
[6] U. Emborg, S. Leth, F. Samuelson, J. Holmgren, Active and passive noise control in practice on the SAAB 2000 high speed turboprop, *AIAA/CEAS Paper 98-2231*, *Fourth AIAA/CEAS Aeroacoustic Conference* (*19th AIAA Aeroacoustics Conference*), Toulouse, France, 1998.
[7] I. Scott, M. Purver, I. Stothers, Tonal active control in production on a large turbo-prop aircraft, *Proceedings of ACTIVE 2002*, Southampton, United Kingdom, 2002, pp. 369–376.
[8] P. Gardonio, Review of active techniques for aerospace vibro-acoustic control, *American Institute of Aeronautics and Astronautics Journal of Aircraft* 39 (2) (2002) 206–214.
[9] L.J. Oswald, Reduction of diesel engine noise inside passenger compartments using active adaptive noise control, *Proceedings of InterNoise* 84 (1984) 483–488.
[10] S.J. Elliott, M. Stothers, P.A. Nelson, A.M. McDonald, D.C. Quinn, T. Saunders, The active control of engine noise inside cars, *Proceedings of InterNoise* 88 (1998) 987–990.
[11] G.P. Mathur, B.N. Tran, M.A. Simpson, Broadband active structural acoustic control of aircraft cabin noise—laboratory tests, *AIAA-97-1636-CP*, 1997.
[12] C. Guigou, C.R. Fuller, Control of aircraft interior broadband noise with foam-PVDF smart skin, *Journal of Sound and Vibration* 220 (3) (1999) 541–557.
[13] T.J. Sutton, S.J. Elliott, A.M. McDonald, Active control of road noise inside vehicles, *Noise Control Engineering Journal* 42 (1994) 137–147.
[14] C. Park, C.R. Fuller, M. Kidner, Evaluation and demonstration of advanced active noise control in a passenger automobile, *Proceedings of Active 2002*, Southampton, United Kingdom, 2002, pp. 275–284.
[15] A. Roure, Self-adaptive broadband active sound control system, *Journal of Sound and Vibration* 101 (3) (1985) 429–441.
[16] C.R. Fuller, S.J. Elliott, P.A. Nelson, *Active Control of Vibration*, 1st Edition, Academic Press, London, 1996.
[17] R.L. Clark, C.R. Fuller, Experiments on active control of structurally radiated sound using multiple piezoceramic actuators, *Journal of the Acoustical Society of America* 91 (6) (1992) 3313–3320.
[18] C.R. Fuller, Active control of sound transmission/radiation from elastic plates by vibration inputs: I—analysis, *Journal of Sound and Vibration* 136 (1) (1990) 1–15.
[19] C.R. Fuller, C.H. Hansen, S.D. Snyder, Active control of sound radiation from a vibrating rectangular panel by sound sources and vibration inputs: an experimental comparison, *Journal of Sound and Vibration* 145 (2) (1991) 195–215.
[20] B.-T. Wang, C.R. Fuller, E.K. Dimitriadis, Active control of noise transmission through rectangular plates using multiple piezoceramic or point force actuators, *Journal of the Acoustical Society of America* 90 (5) (1991) 2820–2830.
[21] F.J. Fahy, *Sound and Structural Vibration*, 1st Edition, Academic Press, London, 1994.
[22] W.L. Li, H.J. Gibeling, Determination of the mutual radiation resistances of a rectangular plate and their impact on the radiated sound power, *Journal of Sound and Vibration* 229 (5) (2000) 1213–1233.
[23] W.L. Li, An analytical solution for the self- and mutual radiation resistances of a rectangular plate, *Journal of Sound and Vibration* 245 (1) (2001) 1–16.
[24] E.J. Skudrzyk, Vibrations of a system with a finite or an infinite number of resonances, *Journal of the Acoustical Society of America* 30 (12) (1958) 1140–1152.
[25] R.A. Burdisso, C.R. Fuller, Dynamic behaviour of structures in feedforward control of sound radiation, *Journal of the Acoustical Society of America* 92 (1) (1992) 277–286.
[26] W.T. Baumann, W.R. Saunders, H.H. Robertshaw, Active suppression of acoustic radiation from impulsively excited structures, *Journal of the Acoustical Society of America* 88 (1991) 3202–3208.
[27] W.T. Baumann, F.-S. Ho, H.H. Robertshaw, Active structural acoustic control of broadband disturbances, *Journal of the Acoustical Society of America* 92 (4) (1992) 1998–2005.
[28] R.L. Clark, C.R. Fuller, A model reference approach for implementing active structural acoustic control, *Journal of the Acoustical Society of America* 92 (3) (1992) 1534–1544.

[29] C.R. Fuller, C.A. Rogers, H.H. Robertshaw, Control of sound radiation with active/adaptive structures, *Journal of the Sound and Vibration* 145 (2) (1992) 19–39.
[30] C.R. Fuller, R.A. Burdisso, A wavenumber domain approach to the active control of structure-borne sound, *Journal of the Sound and Vibration* 148 (2) (1992) 355–360.
[31] R.L. Clark, C.R. Fuller, Active structural acoustic control with adaptive structures including wavenumber considerations, *Journal of Intelligent Material Systems and Structures* 3 (2) (1992) 296–315.
[32] S.J. Elliott, M.E. Johnson, Radiation modes and the active control of sound power, *Journal of the Acoustical Society of America* 94 (4) (1993) 2194–2204.
[33] S.D. Snyder, N. Tanaka, Y. Kikushima, The use of optimally shaped piezoceramic–electric film sensors in the active control of free field structural radiation. Part 1: feedforward control, *American Society of Mechanical Engineers Journal of Vibration and Acoustics* 117 (1996) 311–322.
[34] C.R. Fuller, R.J. Silcox, Active structural acoustic control, *Journal of the Acoustical Society of America* 91 (1) (1992) 519.
[35] M.E. Johnson, S.J. Elliott, Active control of sound radiation using volume velocity cancellation, *Journal of the Acoustical Society of America* 98 (4) (1995) 2174–2186.
[36] C.K. Lee, Theory of laminated piezoceramic plates for the design of distributed sensor/actuators. Part I: Governing equations and reciprocal relationships, *Journal of the Acoustical Society of America* 87 (3) (1990) 1144–1158.
[37] J. Rex, S.J. Elliott, The QWSIS—a new sensor for structural radiation control, *Proceedings of the International Conference on Motion and Vibration Control* (*MOVIC*), Yokohama, 1992, pp. 339–343.
[38] R.L. Clark, C.R. Fuller, R.A. Burdisso, Design approaches for shaping Polyvinylidene Fluoride sensors in active structural acoustic control (ASAC), *Proceedings of the Conference on Recent Advances in Adaptive and Sensory Materials and Their Application*, Blacksburg, VA, 1992, pp. 702–726.
[39] R.L. Clark, C.R. Fuller, Optimal placement of piezoceramic actuators and polyvinylidene fluoride error sensors in active structural acoustic control approaches, *Journal of the Acoustical Society of America* 92 (3) (1992) 1521–1533.
[40] R.L. Clark, C.R. Fuller, Modal sensing of efficient acoustic radiators with polyvinylidene fluoride distributed sensors in active structural acoustic control approaches, *Journal of the Acoustical Society of America* 91 (6) (1992) 3321–3329.
[41] R.A. Burdisso, C.R. Fuller, Optimum actuator and sensor design for active structural acoustic control, *Proceedings of the American Society of Mechanical Engineers Winter Annual Meeting*, New Orleans, LA, ASME AD-35, 1993, pp. 363–370.
[42] M.E. Johnson, S.J. Elliott, Volume velocity sensors for active control, *Proceedings of the Institute of Acoustics* 15 (3) (1993) 411–420.
[43] R.L. Clark, R.A. Burdisso, C.R. Fuller, Design approaches for shaping PVDF sensors in active structural acoustic control, *Journal of Intelligent Material Systems and Structures* 4 (1993) 354–365.
[44] D.M. Carey, F.B. Stulen, Experiments with a two-dimensional multi-modal sensor, *Proceedings of Recent Advances in Active Control of Sound and Vibration*, *Supplement*, 1993, pp. 41–52.
[45] S.A. Collins, D.W. Miller, A.H. von Flotow, Distributed sensors as spatial filters in active structural control, *Journal of Sound and Vibration* 173 (4) (1994) 471–501.
[46] Y. Gu, R.L. Clark, C.R. Fuller, A.C. Zander, Experiments on active control of plate vibration using piezoceramic actuators and polyvinylidene floride (PVDF) modal sensors, *American Society of Mechanical Engineers Journal of Vibration and Acoustics* 116 (1994) 303–308.
[47] M.E. Johnson, Active Control of Sound Transmission, PhD Thesis, University of Southampton, 1996.
[48] F. Charette, A. Berry, C. Guigou, Active control of sound radiation from a plate using a polyvinylidene fluoride volume displacement sensor, *Journal of the Acoustical Society of America* 103 (3) (1998) 1493–1503.
[49] K. Henrioulle, Distributed Actuators and Sensors for Active Noise Control, PhD Thesis, Katholieke Universiteit Leuven, 2001.
[50] R.L. Clark, W.R. Saunders, G.P. Gibbs, *Adaptive Structures*, 1st Edition, Wiley, New York, 1998.
[51] A. Preumont, *Vibration Control of Active Structures*, 2nd Edition, Kluwer Academic Publishers, Dordrecht, 2002.
[52] P. Gardonio, S.J. Elliott, Smart panels for active structural acoustic control, *Proceedings of ISMA 2002*, Katholieke Universiteit Leuven, Belgium, 2002.

[53] S.E. Burke, J.E. Hubbard Jr., Distributed transducer vibration control of thin plates, *Journal of the Acoustical Society of America* 90 (2) (1991) 937–944.
[54] J.P. Maillard, C.R. Fuller, Advanced time domain wave-number sensing for structural acoustic systems. I. Theory and design, *Journal of the Acoustical Society of America* 95 (6) (1994) 3252–3261.
[55] P. Masson, A. Berry, J. Nicolas, Active structural acoustic control using strain sensing, *Journal of the Acoustical Society of America* 102 (3) (1997) 1588–1599.
[56] J.P. Maillard, C.R. Fuller, Comparison of two structural sensing approaches for active structural acoustic control, *Journal of the Acoustical Society of America* 103 (1) (1998) 396–400.
[57] G.P. Gibbs, R.L. Clark, D.E. Cox, J.S. Vipperman, Radiation modal expansion: application to active structural acoustic control, *Journal of the Acoustical Society of America* 107 (1) (2000) 332–339.
[58] A. Preumont, A. Francois, S. Durbru, Piezoceramic array sensing for real-time, broad-band sound radiation measurement, *American Society of Mechanical Engineers Journal of Vibration and Acoustics* 121 (1999) 446–452.
[59] A. Francois, P. De Man, A. Preumont, Piezoceramic array sensing of volume displacement: a hardware demonstration, *Journal of Sound and Vibration* 244 (3) (2001) 395–405.
[60] Y.-S. Lee, P. Gardonio, S.J. Elliott, Volume velocity vibration control of a smart panel using a uniform force actuator and an accelerometer array, *Journal of Smart Materials and Structures* 11 (2002) 863–873.
[61] E.K. Dimitriadis, C.R. Fuller, C.A. Rogers, Piezoceramic actuators for distributed vibration excitation of thin plates, *American Society of Mechanical Engineers Journal of Vibration and Acoustics* 113 (1991) 100–107.
[62] C.A. Rogers, C. Liang, C.R. Fuller, Modelling of shape memory alloy hybrid composites for structural acoustic control, *Journal of the Acoustical Society of America* 89 (1) (1991) 210–220.
[63] R.L. Clark, C.R. Fuller, A.L. Wicks, Characterization of multiple piezoceramic actuators for structural excitation, *Journal of the Acoustical Society of America* 90 (1) (1991) 346–357.
[64] R.L. Clark, M.R. Fleming, C.R. Fuller, Piezoceramic actuators for distributed vibration excitation of thin plates, *American Society of Mechanical Engineers Journal of Vibration and Acoustics* 115 (1993) 332–339.
[65] Su-Wei Zhou, Chen Liang, Craig A. Rogers, Modelling of distributed piezoceramic actuators integrated with thin cylindrical shells, *Journal of the Acoustical Society of America* 96 (3) (1994) 1605–1612.
[66] J.M. Sullivan, J.E. Hubbard Jr., S.E. Burke, Modelling approach for two-dimensional distributed transducers of arbitrary spatial distribution, *Journal of the Acoustical Society of America* 99 (5) (1996) 2965–2974.
[67] J.M. Sullivan, J.E. Hubbard Jr., S.E. Burke, Distributed sensor/actuator design for plates: spatial shape and shading as design parameters, *Journal of Sound and Vibration* 203 (3) (1997) 473–493.
[68] T.J. Sutton, M.E. Johnson, S.J. Elliott, A distributed actuator for the active control of sound transmission through a partition, *Proceedings of the Sixth International Conference on Structural Dynamics Recent Advances*, University of Southampton, United Kingdom, 1997, pp. 1247–1255.
[69] P. Gardonio, Y.-S. Lee, S.J. Elliott, S. Debost, A panel with matched polyvinylidene fluoride volume velocity sensor and uniform force actuator for the active control of sound transmission, *Proceedings of the Institution of Mechanical Engineers* 215 (Part G) (2001) 187–206.
[70] P. Gardonio, Y.-S. Lee, S.J. Elliott, S. Debost, Analysis and measurement of a matched volume velocity sensor and uniform force actuator for active structural acoustic control, *Journal of the Acoustical Society of America* 110 (6) (2001) 3025–3031.
[71] S.E. Burke, J.E. Hubbard Jr., J.E. Meyer, Distributed transducers and collocation, *Mechanical Systems and Signal Processing* 7 (4) (1993) 765–770.
[72] J.Q. Sun, Some observations on physical duality and collocation of structural control sensors and actuators, *Journal of Sound and Vibration* 194 (5) (1996) 765–770.
[73] V. Jayachadran, J.Q. Sun, Unconditional stability domains of structural control systems using dual actuator–sensor pairs, *Journal of Sound and Vibration* 208 (1) (1997) 159–166.
[74] M.J. Balas, Direct velocity feedback of large space structures, *Journal of Guidance and Control* 2 (1979) 252–253.
[75] J.P. Smith, C.R. Fuller, R.A. Burdisso, Active structural acoustic control of radiation due to broadband disturbances, *Journal of the Acoustical Society of America* 92 (4) (1992) 2409–2410.
[76] R.A. Burdisso, J.S. Vipperman, C.R. Fuller, Causality analysis of feedforward-control systems with broadband inputs, *Journal of the Acoustical Society of America* 94 (1) (1993) 234–242.

[77] J.P. Carneal, C.R. Fuller, Active structural acoustic control of noise transmission through double panel systems, *AIAA Paper 93-4421 Presented at 15th American Institute of Aeronautics and Astronautics Aeroacoustics Conference*, Long Beach, CA, 1993.
[78] D.R. Thomas, P.A. Nelson, Feedback control of sound radiation from a plate excited by a turbulent boundary layer, *Journal of the Acoustical Society of America* 98 (5) (1995) 2651–2662.
[79] R.L. Clark, D.E. Cox, Multi-variable structural acoustic control with static compensation, *Journal of the Acoustical Society of America* 102 (5) (1996) 2747–2756.
[80] W. Dehandschutter, K. Henrioulle, J. Swevers, P. Sas, Feedback control of broadband sound radiation using a volume velocity sensor, *Proceedings of ACTIVE 97*, Budapest, Hungary, 1997, pp. 979–992.
[81] D.E. Cox, G.P. Gibbs, R.L. Clark, J.S. Vipperman, Experimental robust control of structural acoustic radiation, *American Society of Mechanical Engineers Journal of Vibration and Acoustics* 121 (1999) 433–439.
[82] J.S. Vipperman, R.L. Clark, Acoustic power suppression of a panel structure using H_∞ output feedback control, *Journal of the Acoustical Society of America* 105 (1) (1999) 219–225.
[83] K. Seto, M. Ren, F. Doi, Modelling and feedback structural acoustic control of a flexible plate, *American Society of Mechanical Engineers Journal of Vibration and Acoustics* 123 (2001) 18–23.
[84] G.C. Smith, R.L. Clark, A crude method of loop-shaping adaptive structures through optimum spatial compensator design, *Journal of Sound and Vibration* 247 (3) (2001) 489–508.
[85] J.K. Henry, R.L. Clark, Active control of sound transmission through a curved panel into a cylindrical enclosure, *Journal of Sound and Vibration* 249 (2) (2002) 325–349.
[86] W. Chang, S.V. Varadan, V.K. Varadan, Design of robust vibration controller for a smart panel using finite element model, *American Society of Mechanical Engineers Journal of Vibration and Acoustics* 124 (2002) 265–276.
[87] J.C. Doyle, K. Glover, P.P. Khargonekar, B.A. Francis, State-space solutions to standard H_2 and H_∞ control problems, *IEEE Transactions on Automatic Control* 34 (8) (1989) 831–847.
[88] S. Boyd, C. Barratt, *Linear Controller Design: Limits of Performance*, Prentice-Hall, Englewood Cliffs, NJ, 1991.
[89] S.D. Snyder, N. Tanaka, Y. Kikushima, The use of optimally shaped piezoceramic-electric film sensors in the active control of free field structural radiation. Part 2: feedback control, *American Society of Mechanical Engineers Journal of Vibration and Acoustics* 118 (1996) 112–121.
[90] P. De Man, A. Francois, A. Preumont, Robust feedback control of a baffled plate via open-loop optimization, *American Society of Mechanical Engineers Journal of Vibration and Acoustics* 124 (2000) 154–157.
[91] B. Bingham, M.J. Atalla, N.W. Hagood, Comparison of structural-acoustic control designs on an active composite panel, *Journal of Sound and Vibration* 244 (5) (2001) 761–778.
[92] C.H. Heatwole, M.A. Franchek, R.J. Bernhard, Robust feedback control of flow-induced structural radiation of sound, *Journal of the Acoustical Society of America* 102 (2) (1997) 989–997.
[93] Y.-S. Lee, P. Gardonio, S.J. Elliott, Coupling analysis of a matched piezoceramic sensor and actuator pair for vibration control of a smart beam, *The Journal of the Acoustical Society of America* 111 (6) (2002) 2715–2726.
[94] D.G. Cole, R.L. Clark, Adaptive compensation of piezoceramic sensori-actuators, *Journal of Intelligent Material Systems and Structures* 5 (1994) 665–672.
[95] P. Gardonio, Y.S. Lee, S.J. Elliott, S. Debost, Active control of sound transmission through a panel with matched PVDF sensor and actuator pair, *Proceedings of Active 99, the 1999 International Symposium on Active Control of Sound and Vibration*, Fort Lauderdale, FL, 1997, pp. 341–354.
[96] S.J. Elliott, *Signal Processing for Active Control*, 1st Edition, Academic Press, London, 2001.
[97] M.E. Johnson, T. Sors, S.J. Elliott, B. Rafaely, Feedback control of broadband sound radiation using a volume velocity sensor, *Proceedings of ACTIVE 97*, Budapest, Hungary, 1997, pp. 1007–1020.
[98] T.C. Sors, S.J. Elliott, Modelling and feedback control of sound radiation from a vibrating panel, *Smart Material Structures* 8 (1999) 301–314.
[99] C. Guigou, C.R. Fuller, Adaptive feedforward and feedback methods for active/passive sound radiation control using smart foam, *Journal of the Acoustical Society of America* 104 (1) (1998) 226–231.
[100] B. Petitjean, I. Legrain, Feedback controllers for active vibration suppression, *Journal of Structural Control* 3 (1–2) (1996) 111–127.
[101] B. Petitjean, I. Legrain, F. Simon, S. Pauzin, Active control experiments for acoustic radiation reduction of a sandwich panel: feedback and feedforward investigations, *Journal of Sound and Vibration* 252 (1) (2002) 19–36.

[102] P. Gardonio, S.J. Elliott, Driving point and transfer mobility matrices for thin plates excited in flexure, ISVR Technical Report No. 277, 1999.
[103] G.B. Warburton, *The Dynamical Behaviour of Structures*, Pergamon Press, New York, 1976.
[104] D.J. Nefske, S.H. Sung, Sound in small enclosures, in: L.L. Beranek, I.L. Ver (Eds.), *Noise and Vibration Control Engineering*, Wiley, USA, 1992 (Chapter 6).
[105] E. Bianchi, P. Gardonio, S.J. Elliott, Smart panel with an array of decentrlized control systems for active structural acoustic control, ISVR Technical Memorandum No. 886, 2002.
[106] S.S. Rao, *Vibration Measurement and Applications, Mechanical Vibration*, Addison-Wesley, Reading, MA, USA, 1995 (Chapter 10).